

NLO QCD Analysis of Polarized Deep Inelastic Scattering

Elliot Leader

Department of Physics

Birkbeck College, University of London

Malet Street, London WC1E 7HX, England

E-mail: e.leader@physics.bbk.ac.uk

Aleksander V. Sidorov

Bogoliubov Theoretical Laboratory

Joint Institute for Nuclear Research

141980 Dubna, Russia

E-mail: sidorov@thsun1.jinr.dubna.su

Dimiter B. Stamenov

Institute for Nuclear Research and Nuclear Energy

Bulgarian Academy of Sciences

Blvd. Tsarigradsko chaussee 72, Sofia 1784, Bulgaria

E-mail: stamenov@inrne.acad.bg

Abstract

We have carried out a NLO analysis of the world data on polarized DIS in the \overline{MS} scheme. We have studied two models of the parametrizations of the input parton densities, the first due to Brodsky, Burkhardt and Schmidt (BBS) which gives a simultaneous parametrization for both the polarized and unpolarized densities and in which the counting rules are strictly imposed, the second in which the input polarized densities are written in terms of the unpolarized ones in the generic form $\Delta q(x) = f(x)q(x)$ with $f(x)$ some simple smooth function. In both cases a good fit to the polarized data is achieved. As expected the polarized data do not allow a precise determination of the polarized gluon density. Concerning the polarized sea-quark densities, these are fairly well determined in the BBS model because of the interplay of polarized and unpolarized data, whereas in the second model, where only the polarized data are relevant, the polarized sea-quark densities are largely undetermined.

1. Introduction.

Experiments on polarized deep inelastic scattering (DIS) were initiated at SLAC by the SLAC-Yale group [1] soon after the discovery of Bjorken scaling. Enormous impetus was given to the subject by the European Muon Collaboration (EMC) experiment at CERN [2] in 1988 whose results seemed to imply a "spin crisis in the parton model" [3]. Much theoretical and experimental work has followed and today there is a rich program of experiments under way (E154, E155 at SLAC; HERMES at HERA) or in the progress of being set up (COMPASS at CERN).

Experiments on unpolarized DIS provide information on the unpolarized quark densities $q(x, Q^2)$ and gluon density $G(x, Q^2)$ inside a nucleon. Polarized DIS experiments, using a longitudinally polarized target, give us more detailed information, namely the number densities of quarks $q(x, Q^2)_\pm$ and gluons $G(x, Q^2)_\pm$ whose helicity is respectively along or opposite to the helicity of the parent nucleon. The usual densities are

$$q(x, Q^2) = q_+(x, Q^2) + q_-(x, Q^2) , \quad G(x, Q^2) = G_+(x, Q^2) + G_-(x, Q^2) \quad (1)$$

and the new information is then contained in the polarized structure function $g_1(x, Q^2)$ which is expressed in terms of the *polarized* parton densities

$$\Delta q(x, Q^2) = q_+(x, Q^2) - q_-(x, Q^2) , \quad \Delta G(x, Q^2) = G_+(x, Q^2) - G_-(x, Q^2) . \quad (2)$$

Two developments in the past few years have made it possible and worthwhile to attempt a detailed comparative study of the polarized parton distributions. On the one hand, a wealth of new data, much of it high quality, has appeared [4 - 12]. On the other, the theoretical calculation of the Altarelli-Parisi splitting functions to two-loop order has been, after several hiccoughs, completed successfully [13].

It would be wrong, however, to imagine that the polarized densities can now be determined to the same accuracy with which the unpolarized densities are known. This can be understood quite simply. Up to the present the polarized data consist solely of fully inclusive neutral current (in effect, photon induced) reactions on protons and (via deuterium or Helium-3) on neutrons, *i.e.* one has information on the two polarized structure functions $g_1^p(x, Q^2)$ and $g_1^n(x, Q^2)$. Even if one makes some simplifying assumptions about the polarized sea, e.g. $\Delta\bar{u}(x) = \Delta\bar{d}(x) = \Delta\bar{s}(x)$ or $\Delta\bar{u}(x) = \Delta\bar{d}(x) = 2\Delta\bar{s}(x)$ one is still expressing two experimental functions in

terms of four densities: $\Delta u(x, Q^2)$, $\Delta d(x, Q^2)$, $\Delta \bar{q}(x, Q^2)$ and $\Delta G(x, Q^2)$. What is lacking here is the information from charged current reactions which plays an important role in pinning down the unpolarized densities. The situation is alleviated by the beautiful connection between the first moments of the polarized parton densities and weak interaction physics. Namely, one has the connection with neutron β -decay, via the Bjorken sum rule,

$$\int_0^1 dx [\Delta u(x, Q^2) + \Delta \bar{u}(x, Q^2) - \Delta d(x, Q^2) - \Delta \bar{d}(x, Q^2)] = g_A/g_V \quad (3)$$

and, to the extent that flavour $SU(3)$ is a good symmetry, the connection with hyperon β -decay

$$\int_0^1 dx \{ \Delta u(x, Q^2) + \Delta \bar{u}(x, Q^2) + \Delta d(x, Q^2) + \Delta \bar{d}(x, Q^2) - 2[\Delta s(x, Q^2) + \Delta \bar{s}(x, Q^2)] \} = 3F - D. \quad (4)$$

The values of g_A/g_V and 3F-D are taken from [14]

$$g_A/g_V = 1.2573 \pm 0.0028, \quad 3F - D = 0.579 \pm 0.025. \quad (5)$$

Assuming a roughly flavour-independent polarized sea, allows one to interpret Eqs. (3) and (4) as statements about the first moments of the polarized valence densities:

$$\int_0^1 dx [\Delta u_v(x, Q^2) - \Delta d_v(x, Q^2)] \cong 1.26, \quad (6)$$

$$\int_0^1 dx [\Delta u_v(x, Q^2) + \Delta d_v(x, Q^2)] \cong 0.58, \quad (7)$$

which immediately suggests that $\Delta d_v(x, Q^2)$ is of opposite sign to $\Delta u_v(x, Q^2)$ and of roughly comparable magnitude, in agreement with simple $SU(6)$ models of the proton wave-function. Eqs. (3) and (4) are crucial supplements to the polarized DIS data.

In seeking input parametrizations of the polarized densities into the QCD evolution equations one must clearly respect the positivity of the number densities $q(x, Q_0^2)_\pm$, which *via* (1) and (2) is equivalent to demanding

$$|\Delta q(x, Q_0^2)| \leq q(x, Q_0^2) \quad (8)$$

There are, in addition, certain *counting rules* relating to the behaviour of $\Delta q(x)/q(x)$ as $x \rightarrow 0$ and $x \rightarrow 1$, which follow in the parton model from perturbative QCD and

the form of the infinite momentum frame nucleon wave function [15 - 17].

We have examined two classes of models for the input densities. The first, due to Brodsky, Burkardt and Schmidt [17] is unusual since it directly parameterizes $q_+(x, Q^2)$ and $q_-(x, Q^2)$ at some $Q^2 = Q_0^2$ (rather than $\Delta q(x, Q_0^2)$ and $q(x, Q_0^2)$) so that the free parameters are determined from a simultaneous fit to the polarized and unpolarized data. Positivity is simple to implement and the counting rules are imposed exactly at $Q^2 = Q_0^2$.

In the second, each polarized parton distribution is written in the generic form $\Delta q(x, Q_0^2) = f(x)q(x, Q_0^2)$ at some Q_0^2 , with the usual densities $q(x, Q_0^2)$ determined from the unpolarized data (in practice we utilize the MRS(A') set of distributions [18]). The functions $f(x)$ are parameterized so as to respect positivity but the counting rules are not imposed in a strict fashion.

Finally it should be remembered that beyond the leading order in perturbation theory the parton densities become scheme dependent. In this paper we work in the \overline{MS} scheme.

In Section 2 we wish to draw the reader's attention to certain interesting qualitative features of the polarized DIS data. In Section 3 we explain the method of analysis and in Section 4 discuss the parametrization of the models and their properties. Our results are presented and analyzed in Section 5 and conclusions follow in Section 6.

2. Implications of qualitative features of the data

The structure functions $g_1^{p,n}(x, Q^2)$ are determined in the following x range: $0.003 < x < 0.8$. For small x there are large errors on the measured values, but if one takes the central values of the data points as indication of the trend of the behaviour as $x \rightarrow 0$ then one is led to some surprising conclusions. To see this, consider the expressions for the structure functions $g_1^{p,n}(x, Q^2)$. They can be expressed in terms of contributions $\Delta q_3(x, Q^2)$, $\Delta q_8(x, Q^2)$ and $\Delta \Sigma(x, Q^2)$ of definite flavour symmetry as

$$g_1^{p,n}(x, Q^2) = \left\{ \pm \frac{1}{12} \Delta q_3(x, Q^2) + \frac{1}{36} \Delta q_8(x, Q^2) + \frac{1}{9} \Delta \Sigma(x, Q^2) \right\} \{1 + O(\alpha_s)\} \quad (9)$$

where the flavour non-singlet contributions are

$$\Delta q_3(x, Q^2) = \Delta u(x, Q^2) + \Delta \bar{u}(x, Q^2) - \Delta d(x, Q^2) - \Delta \bar{d}(x, Q^2), \quad (10)$$

$$\begin{aligned} \Delta q_8(x, Q^2) = \Delta u(x, Q^2) + \Delta \bar{u}(x, Q^2) &+ \Delta d(x, Q^2) + \Delta \bar{d}(x, Q^2) \\ &- 2[\Delta s(x, Q^2) + \Delta \bar{s}(x, Q^2)] \end{aligned} \quad (11)$$

and the singlet contribution is

$$\Delta\Sigma(x, Q^2) = \sum_f [\Delta q_f(x, Q^2) + \Delta\bar{q}_f(x, Q^2)] . \quad (12)$$

The gluon contribution to $g_1(x, Q^2)$ is hidden in the $O(\alpha_s)$ correction terms in (9) and a more precise expression will be given in Eq. (18).

One sees then that the difference $g_1^p(x, Q^2) - g_1^n(x, Q^2)$ is a purely non-singlet, whereas the sum $g_1^p(x, Q^2) + g_1^n(x, Q^2)$ is a mixture of singlet and non-singlet contributions.

Now according either to the small- x behaviour of the evolution equations [19] or to the summation of double logarithmic terms at small x [20], the singlet contribution should dominate over the non-singlet terms as $x \rightarrow 0$, which, by the above, could imply $(g_1^p + g_1^n) > (g_1^p - g_1^n)$ at small x . The data (see Fig. 1) show precisely the opposite trend. However, while the theoretical arguments predict the form of the behaviour as $x \rightarrow 0$, namely $C_{ns}x^{-a_{ns}}$ or $C_sx^{-a_s}$ with $a_s > a_{ns} > 0$, the values of the coefficients C_{ns} , C_s are sensitive to the structure of the parton distributions at Q_0^2 . So there need not be a contradiction at presently measured x -values. However, as experiments probe smaller and smaller x , there ought to be a dramatic change in the trend of the data or else the theoretical arguments are incomplete.

On a practical level concerning the present data, the behaviour in Fig. 1 can lead to difficulties when one makes, as one is forced to do, some simplifying assumption for the polarized sea, such as $\Delta\bar{u}(x, Q_0^2) = \Delta\bar{d}(x, Q_0^2)$. For then $\Delta q_3(x, Q^2)$ in (10) practically depends only on valence distributions and in some cases one finds that the best-fit parameters tend to make $\Delta d_v(x, Q^2)$ so large and negative at small x that positivity is violated.

3. Method of analysis

Measurements of polarized deep inelastic lepton nucleon scattering yield *direct* information on the virtual photon- nucleon asymmetry $A_1^N(x, Q^2)$. Neglecting as usual the subdominant contributions, $A_1^N(x, Q^2)$ can be expressed *via* the polarized structure function $g_1^N(x, Q^2)$ as

$$A_1^N(x, Q^2) \cong \frac{g_1^N(x, Q^2)}{F_1^N(x, Q^2)} = \frac{g_1^N(x, Q^2)}{F_2^N(x, Q^2)} [2x(1 + R^N(x, Q^2))] , \quad (13)$$

where

$$R^N = (F_2^N - 2xF_1^N)/2xF_1^N \quad (14)$$

and F_1^N and F_2^N are the unpolarized structure functions.

Usually the theoretical analysis of the data is presented in terms of $g_1^N(x, Q^2)$ extracted from the measured values of $A_1^N(x, Q^2)$ according to (13) using different parametrizations of the experimental data for F_2 and R . The parametrizations [21] of F_2 and [22] of R were used in the most recent analyses. Some experimental groups assume also Q^2 scaling of $A_1^N(x, Q^2)$ in their extraction of $g_1^N(x, Q^2)$. However, bearing in mind the recent NLO calculations of g_1 in QCD, this assumption is not theoretically correct, especially in the small x region.

In our analysis we follow the approach first used in [23], in which the next-to-leading (NLO) QCD predictions for the spin-asymmetry $A_1^N(x, Q^2)$ are confronted with the *directly measured* values of $A_1^N(x, Q^2)$ rather than with the $g_1^N(x, Q^2)$ derived by the procedure mentioned above. A further advantage of such an approach is that higher twist contributions are expected to partly cancel in the ratio (13), in contrast to the situation for $g_1^N(x, Q^2)$. Usually to avoid the influence of higher twist effects Q^2 -cuts in the (x, Q^2) data set are introduced. Bearing in mind that in polarized DIS most of the small x data points are at low Q^2 , a lower than usual cut is needed ($Q^2 > 1 \text{ GeV}^2$) in order to have enough data for a theoretical analysis. We consider that in this approach such a low Q^2 -cut is more reasonable.

In NLO approximation

$$A_1^N(x, Q^2)_{NLO} \cong \frac{2xg_1^N(x, Q^2)_{NLO}}{2xF_1^N(x, Q^2)_{NLO}}. \quad (15)$$

In (15) $N = p$, n and $d = (p + n)/2$.

To calculate $g_1^N(x, Q^2)$ and $2xF_1^N(x, Q^2)$ we have used the analytic NLO solutions for the moments in Mellin space with the n th moment being defined by

$$M_n^N(Q^2) = \int_0^1 dx x^{n-2} x g_1^N(x, Q^2), \quad n = 1, 2, \dots \quad (16)$$

$$\overline{M}_n^N(Q^2) = \int_0^1 dx x^{n-2} 2xF_1(x, Q^2), \quad n = 2, 3, \dots \quad (17)$$

In NLO approximation with $n_f = 3$ active flavours the moments (16) of the structure function $g_1^N(x, Q^2)$ can be written in the form [24]:

$$\begin{aligned} M_n^{p(n)}(Q^2) &= \left\{ \pm \frac{1}{12} \Delta q_3(n, Q^2) + \frac{1}{36} \Delta q_8(n, Q^2) + \frac{1}{9} \Delta \Sigma(n, Q^2) \right\}_{NLO} \\ &+ \frac{\alpha(Q^2)}{2\pi} \delta C_n^q \left\{ \pm \frac{1}{12} \Delta q_3(n, Q^2) + \frac{1}{36} \Delta q_8(n, Q^2) + \frac{1}{9} \Delta \Sigma(n, Q^2) \right\}_{LO} \\ &+ \frac{\alpha(Q^2)}{2\pi} \delta C_n^G \Delta G(n, Q^2)_{LO}, \end{aligned} \quad (18)$$

$$M_n^d(Q^2) = \frac{1}{2}[M_n^{(p)}(Q^2) + M_n^{(n)}(Q^2)](1 - 1.5\omega_D) . \quad (19)$$

where Δ_{q_3} , Δ_{q_8} and $\Delta\Sigma$ are the moments of the flavour non-singlet and singlet combinations (10), (11) and (12), respectively, while $G(n, Q^2)$ denotes the moments of the gluon density $G(x, Q^2)$. The subscript "LO" in (18) means that the moments of the corresponding densities satisfy the LO Q^2 -evolution equations, in which for the strong coupling constant $\alpha_s(Q^2)$ the NLO approximation

$$\frac{\alpha_s(Q^2)}{4\pi} = \frac{1}{\beta_0 \ln Q^2 / \Lambda^2} - \frac{\beta_1 \ln \ln Q^2 / \Lambda^2}{\beta_0^3 \ln Q^2 / \Lambda^2} \quad (20)$$

is taken. In (19) for the probability of the deuteron to be in D-state we have taken $\omega_d = 0.05 \pm 0.01$, which covers most of the published values [25].

All quantities - the anomalous dimensions $\delta\gamma_{ij}^n$ up to two-loop approximation and the moments of the coefficient functions δC_n^q and δC_n^G in one-loop approximation needed to derive the analytic "LO" and NLO solutions for the moments of the parton densities, can be found, for instance, in [23].

Unlike paper [23] where the expressions for the moments of g_1 and $2xF_1$ are numerically Mellin-inverted to yield the structure functions in Bjorken x -space, we follow a method [26, 27] which presents the structure functions *analytically*. Having the NLO Q^2 -evolution of the moments (18) and (19) we can write the structure function $g_1(x, Q^2)_{NLO}$ in the form:

$$xg_1^N(x, Q^2) = x^\alpha(1-x)^\beta \sum_{n=0}^{N_{max}} \Theta_n^{\alpha, \beta}(x) \sum_{j=0}^n c_j^{(n)}(\alpha, \beta) M_{j+2}^{NS}(Q^2), \quad (21)$$

where $\Theta_n^{\alpha, \beta}(x)$ is a set of Jacobi polynomials and $c_j^{(n)}(\alpha, \beta)$ are coefficients of the series of $\Theta_n^{\alpha, \beta}(x)$ in powers in x :

$$\Theta_n^{\alpha, \beta}(x) = \sum_{j=0}^n c_j^{(n)}(\alpha, \beta) x^j. \quad (22)$$

N_{max} , α and β have to be chosen so as to achieve the fastest convergence of the series on the R.H.S. of Eq. (21) and to reconstruct xg_1 with the required accuracy. We use $\alpha = 0.7$, $\beta = 3.0$ and $N_{max} = 8$. These values guarantee an accuracy better than 2.5% in the experimental x range: $0.01 \leq x < 0.8$ and better than 5% for smaller x .

The same method has been applied to calculate the unpolarized structure functions $2xF_1^N(x, Q^2)_{NLO}$ from their moments (17). Following the results of Ref. [27] we use for the quantities N_{max} , α and β in this case:

$$N_{max} = 12, \quad \alpha = -0.85, \quad \beta = 3.0$$

in order to guarantee an accuracy better than 10^{-3} in the x range mentioned above. In the present calculations of $2xF_1$ the MRS(A') parametrization for the input unpolarized parton densities has been used.

As already mentioned in the introduction all calculations are performed in \overline{MS} scheme. In this scheme the first moment of the Wilson coefficient function $\delta C_1^G = 0$, so the axial anomaly contribution of $\Delta G(1, Q^2)$ to the first moment $M_1^N(Q^2) \equiv \Gamma_1^N(Q^2)$ of $g_1(x, Q^2)$ vanishes, *i.e.* the singlet axial charge $a_0(Q^2)$ coincides with $\Delta\Sigma(1, Q^2)$ (twice the total helicity) carried by the quarks in the nucleon. In the present study we use the \overline{MS} scheme because of our choice of the input parton distributions (see, Eqs. (31) and (35)). A NLO analysis of the polarized DIS data in a renormalization scheme, which allows for an anomalous gluonic contribution $\Delta G(1, Q^2)$ to the Ellis-Jaffe sum rule [28] is presented in [29].

The value of $\Lambda_{\overline{MS}}$ is taken to be $\Lambda_{\overline{MS}}(n_f = 3) = 284 \text{ MeV}$. This value corresponds to $\Lambda_{\overline{MS}}(n_f = 4) = 231 \text{ MeV}$ [18] according to the requirement α_s be continuous across each threshold $Q^2 \geq m_q^2$. The contributions of charmed quarks to $g_1(x, Q^2)$ is assumed to be negligible at present energies [30] and will not be considered in our analysis.

The last step before fitting the theoretical predictions for $A_1(x, Q^2)$ to the data is to choose the input polarized parton densities at some fixed value of $Q^2 = Q_0^2$, evolve them to Q^2 and then put them into (21).

4. Models for the input parton distributions

We have studied two classes of models:

(a) the model of Brodsky, Burkardt and Schmidt (BBS) [17], which directly parametrizes the parton densities $q_{\pm}(x)$ and which respects the perturbative QCD counting rules exactly

(b) an example of parametrization of the form $\Delta q(x) = f(x)q(x)$ where $q(x)$ are the unpolarized parton densities of Martin, Roberts and Stirling MRS(A') [18] and in which the counting rules are somewhat relaxed.

(a) *The BBS counting rule model*

It is well known that the valence Fock states with the minimum numbers of constituents dominate in determining the behaviour of the unpolarized valence distributions $u_v(x)$, $d_v(x)$ in the region $x \rightarrow 1$ and this leads [31], *via* perturbative QCD, to the prediction

$$u_v(x), d_v(x) \sim (1-x)^3 \quad (x \rightarrow 1). \quad (23)$$

The same arguments applied to the polarized case suggest [15, 17] that

$$q_{v+}(x) \sim (1-x)^3, \quad q_{v-}(x) \sim (1-x)^5 \quad (x \rightarrow 1) \quad (24)$$

implying, *via* (23), that

$$\frac{\Delta q_v(x)}{q_v(x)} \rightarrow 1 \quad (x \rightarrow 1). \quad (25)$$

Simple perturbative arguments based upon the splitting functions for $q \rightarrow qG$ and $G \rightarrow q\bar{q}$ can then be used to predict the behaviour of the gluon and sea densities generated from the valence quarks in the region $x \rightarrow 1$, namely [16, 17]

$$G(x) \sim (1-x)^4, \quad \frac{\Delta G(x)}{G(x)} \rightarrow 1 \quad (x \rightarrow 1) \quad (26)$$

and

$$\bar{q}(x) \sim (1-x)^5, \quad \frac{\Delta \bar{q}}{\bar{q}} \rightarrow 1 \quad (x \rightarrow 1). \quad (27)$$

Unfortunately these simple sum rules are not compatible with the evolution equations. If they hold at some Q_0^2 then the power of $(1-x)$ involved will grow like $\ln \ln Q^2$ at large Q^2 . It is therefore not clear to what extent the above rules should hold at some Q_0^2 at which one chooses to parameterize the parton densities. Presumably they should be more accurate at momentum scales $Q_0 \sim \Lambda_{QCD}$, so that for the typical values of Q_0^2 utilized in the data analyses, $1 \leq Q_0^2 \leq 4 \text{ GeV}^2$, one might expect somewhat higher powers of $(1-x)$ to appear. Indeed, analyses of the unpolarized data yield typically, at $Q_0^2 = 4 \text{ GeV}^2$,

$$u_v(x) \sim (1-x)^{(3-4)}, \quad d_v(x) \sim (1-x)^{(4-5)} \quad (28)$$

somewhat at variance with (23) and with the faster decrease of $d_v(x)$ being related to the experimentally established behaviour of $F_2^n(x)/F_2^p(x)$ as $x \rightarrow 1$.

The BBS model is interesting because it asks how well the data can be fitted if the exact conditions (23 - 27) are imposed.

Concerning the behaviour as $x \rightarrow 0$, perturbative arguments based on the splitting functions predict [17] that the gluons and antiquarks

$$\frac{\Delta\bar{q}(x)}{\bar{q}(x)}, \quad \frac{\Delta G(x)}{G(x)} \rightarrow \text{const.}x \quad (x \rightarrow 0). \quad (29)$$

This behaviour is consistent with Regge-type arguments.

For the gluons BBS use wave-function arguments to suggest that the *const* in (29) is approximately equal to 1 and their gluon density automatically satisfies this constraint. For the sea the *const* is determined by the fit to the data.

In the original BBS paper [17] an analysis of the polarized data then available and a fit to the MRS(D0') parametrization of the unpolarized data were performed, but without taking account of the corrections from QCD evolution. As on the one hand, there is now much more polarized data available, especially at smaller x , and the MRS(D0') fit has been superseded by other parametrizations which fit the unpolarized low- x data far better, and on the other, the NLO calculations in QCD have been completed, we have felt it important to examine to what extent the original claims of the BBS model remain valid.

The input helicity-dependent parton densities at Q_0^2 in the BBS model have the following form:

$$\begin{aligned} x(\Delta u(x) + \Delta\bar{u}(x)) &= x^{1-\alpha_q}(1-x)^3[A_u + B_u(1-x) - C_u(1-x)^2 - D_u(1-x)^3], \\ x(\Delta d(x) + \Delta\bar{d}(x)) &= x^{1-\alpha_q}(1-x)^3[A_d + B_d(1-x) - C_d(1-x)^2 - D_d(1-x)^3], \\ x(\Delta s(x) + \Delta\bar{s}(x)) &= x^{1-\alpha_q}(1-x)^5[A_s + B_s(1-x) - C_s(1-x)^2 - D_s(1-x)^3], \\ x\Delta G(x) &= x^{1-\alpha_g}(1-x)^4[A_g + B_g(1-x)][1 - (1-x)^2], \end{aligned} \quad (30)$$

while the unpolarized parton densities at Q_0^2 are given as

$$\begin{aligned} x(u(x) + \bar{u}(x)) &= x^{1-\alpha_q}(1-x)^3[A_u + B_u(1-x) + C_u(1-x)^2 + D_u(1-x)^3], \\ x(d(x) + \bar{d}(x)) &= x^{1-\alpha_q}(1-x)^3[A_d + B_d(1-x) + C_d(1-x)^2 + D_d(1-x)^3], \\ x(s(x) + \bar{s}(x)) &= x^{1-\alpha_q}(1-x)^5[A_s + B_s(1-x) + C_s(1-x)^2 + D_s(1-x)^3], \\ xG(x) &= x^{1-\alpha_g}(1-x)^4[A_g + B_g(1-x)][1 + (1-x)^2]. \end{aligned} \quad (31)$$

The constraints

$$A_q + B_q = C_q + D_q \quad (32)$$

are imposed on the constants A_q , B_q , C_q and D_q in (30) and (31) in order to ensure the convergence of the helicity-dependent sum rules (3) and (4). Thus in the BBS model

the Regge behaviour of the polarized quark densities $\Delta q \sim x^{-\alpha_R}$ is automatically one unit less than the unpolarized intercept α_q : $\alpha_R = \alpha_q - 1$. Isospin symmetry at low x requires

$$A_u + B_u + C_u + D_u = A_d + B_d + C_d + D_d . \quad (33)$$

If in addition to (32) and (33) the helicity- dependent sum rules (3) and (4) and the energy-momentum sum rule for the unpolarized densities (31) are taken into account, the number of the unknown parameters associated with the input polarized densities is reduced to $N = 16 - 7 = 9$. These free parameters - we have chosen

$$\{B_u, C_u, D_u, C_d, C_s, D_s, B_g, \alpha_q, \alpha_g\} , \quad (34)$$

are determined by a *simultaneous* fit of the theoretical predictions (15) and the BBS *unpolarized* parton densities (31) to the world $A_1^N(x, Q^2)$ data and the MRS(A') set of unpolarized parton densities, respectively. We recall that the MRS(A') densities at next-to-leading order are parameterized at $Q_0^2 = 4 \text{ GeV}^2$ and are well determined from the wide set of unpolarized experiments. Note that the choice of unpolarized densities is not crucial for the present analysis.

(b) *Models based on the unpolarized parton densities*

We have also analyzed the polarized DIS data using the following expressions for the input polarized parton distributions at Q_0^2

$$\begin{aligned} x\Delta u_v(x, Q_0^2) &= \eta_u A_u x^{a_u} x u_v(x, Q_0^2) , \\ x\Delta d_v(x, Q_0^2) &= \eta_d A_d x^{a_d} x d_v(x, Q_0^2) , \\ x\Delta Sea(x, Q_0^2) &= \eta_s A_s x^{a_s} x Sea(x, Q_0^2) , \\ x\Delta G(x, Q_0^2) &= \eta_g A_g x^{a_g} (1-x)^{b_g} x G(x, Q_0^2) \end{aligned} \quad (35)$$

where on R.H.S. of (35) we use the MRS(A') unpolarized densities. The normalization factors A_f are determined in such a way as to ensure that the first moments of the polarized densities are given by η_f . Since the present polarized experiments do not allow for a flavour decomposition of the sea, SU(3) symmetry of the sea-quark densities is assumed

$$\Delta\bar{u}(x, Q_0^2) = \Delta\bar{d}(x, Q_0^2) = \Delta\bar{s}(x, Q_0^2) = \Delta\bar{q}(x, Q_0^2) . \quad (36)$$

Following this assumption $\Delta Sea(x, Q_0^2) = 6\Delta\bar{q}(x, Q_0^2)$ and $\eta_s = 6\eta_{\bar{q}}$, where $\eta_{\bar{q}}$ is the first moment of $\Delta\bar{q}$. Note also that the very small charm contribution to the unpolarized sea on R.H.S. of (35) is ignored in our analysis.

In this approach, the first moments of the valence quark densities η_u and η_d are obtained directly from the sum rules (6) and (7)

$$\eta_u = 0.918, \quad \eta_d = -0.339 . \quad (37)$$

The first moment of the polarized sea η_s is fixed from the measured value of Γ_1 . More details are discussed in the next section. The rest of the parameters

$$\{a_u, a_d, a_s, \eta_g, a_g, b_g\} , \quad (38)$$

have to be determined from the fit to the $A_1^N(x, Q^2)$ data.

Finally it should be noted that using a set of polarized parton densities like (35), $\Delta d_v(x, Q_0^2)$ and $\Delta \bar{q}(x, Q_0^2)$ will turn out to be negative in the whole x region in contrast to the BBS model where these quantities become positive at large x .

5. Results of Analysis

In this section we present the results of our fits to the world $A_1^N(x, Q^2)$ data: EMC proton data [2], SLAC E142 neutron data [4], SLAC E143 proton and deuteron data [5 - 7], SMC proton data [9] and the SMC deuteron data [12] which are combined data from the 1992 [10], 1994 [11] and 1995 runs. The data used (203 experimental points) cover the following kinematic region:

$$0.004 < x < 0.75, \quad 1 < Q^2 < 72 \text{ GeV}^2 . \quad (39)$$

We have chosen $Q_0^2 = 4 \text{ GeV}^2$. In all fits only statistical errors are taken into account. "Higher twist" corrections are not included in the present study. As already discussed above, in the approach used their effect is expected to be negligible.

(a) BBS model

A comparison of our results (solid curves) with the data on $A_1^N(x, Q^2)$ is shown in Figs. 2a - 2f. Our NLO results for $g_1^N(x, Q^2)$ are illustrated in Fig. 7. The minimum of the functional χ^2 is achieved at $\chi^2 = 232.7$ and $\chi^2/DOF = 232.7/194 = 1.20$. The values of the free input parton parameters (34) corresponding to this χ^2 value are

$$\begin{aligned} B_u &= -3.010 \pm 0.156, & C_u &= 2.143 \pm 0.137, & D_u &= -2.065 \pm 0.148 , \\ C_d &= 1.689 \pm 0.227, & C_s &= 0.334 \pm 0.044, & D_s &= -0.292 \pm 0.042 , \\ B_g &= -0.339 \pm 0.454, & \alpha_q &= 1.313 \pm 0.056, & \alpha_g &= 1.233 \pm 0.073 . \end{aligned} \quad (40)$$

The rest of the parameters $A_u, A_d, B_d, D_d, A_s, B_s$ and A_g are determined by the constraints (32) and (33), the sum rules (3) and (4) and the momentum-energy sum rule, giving

$$\begin{aligned} A_u = 3.088, \quad A_d = 0.343, \quad B_d = -0.265, \quad D_d = -1.610, \\ A_s = 0.001, \quad B_s = 0.041, \quad A_g = 1.019. \end{aligned} \quad (41)$$

It is seen from Figs. 2a - 2f that the NLO QCD predictions using the BBS model for the input parton distributions are in a good agreement with the presently available data on $A_1^N(x, Q^2)$, as well as with the corresponding $g_1^N(x, Q^2)$ data (see Fig. 7).

For the first moments of the polarized flavour and flavour-singlet distributions at $Q_0^2 = 4 \text{ GeV}^2$ we obtain

$$\Delta u + \Delta \bar{u} = 0.839, \quad \Delta d + \Delta \bar{d} = -0.405, \quad 2\Delta \bar{s} = -0.079, \quad (42)$$

and

$$\Delta \Sigma = a_0 = 0.342. \quad (43)$$

These values yield for the quantity $\Gamma_1^N(Q^2)$, the first moment of g_1^N ,

$$\Gamma_1^p(5 \text{ GeV}^2) = 0.146, \quad \Gamma_1^n(5 \text{ GeV}^2) = -0.047, \quad \Gamma_1^d(5 \text{ GeV}^2) = 0.046, \quad (44)$$

which are in a good agreement with their experimental values

$$\begin{aligned} \Gamma_1^p(5 \text{ GeV}^2) &= 0.141 \pm 0.011 \quad (\text{All proton data}), \\ \Gamma_1^d(5 \text{ GeV}^2) &= 0.039 \pm 0.004 \quad (\text{All deuteron data}). \end{aligned} \quad (45)$$

The experimental values of Γ_1^p and Γ_1^d in (45) have been determined in [9] and [12] by combining SMC and SLAC E143 results on A_1^p and A_1^d , respectively.

Our result for the axial charge a_0

$$a_0(5 \text{ GeV}^2) = \Delta \Sigma(5 \text{ GeV}^2) = 0.341 \quad (46)$$

is also in a good agreement with its experimental value $a_0(5 \text{ GeV}^2) = 0.29 \pm 0.06$ recently determined [9] from the combined analysis of all proton, neutron and deuteron data.

We obtain for the small x behaviour of the input sea quark and gluon distributions

$$x\Delta\bar{q}(x) \sim x^{0.69}, \quad x\Delta G(x) \sim x^{0.77}. \quad (47)$$

This result confirms that of Gehrmann and Stirling [32] who used in their NLO analysis the same renormalization scheme and the same Q_0^2 , but different input parton densities.

It is well known that in the unpolarized case the gluon distribution can not be well determined by the fit to the data on nucleon structure functions alone. The situation in the polarized DIS is even worse. In particular, the fact that the parameter B_g in (40) is not well determined reflects this uncertainty in the extraction of $\Delta G(x, Q^2)$ from the data. We obtain for the first moment of $\Delta G(x, Q^2)$: $\Delta G_1(4 \text{ GeV}^2) = 0.447$, which does not coincide with the mean values of this quantity given in most of the theoretical analyses. This result for $\Delta G_1(Q_0^2)$ is not surprising. It should be noted that in the BBS model one can show that $\Delta G_1(Q_0^2)$ is constrained by

$$\Delta G_1(Q_0^2) < 2G_2(Q_0^2) - G_3(Q_0^2) , \quad (48)$$

where $G_2(Q_0^2)$ and $G_3(Q_0^2)$ are the second and third moments of the unpolarized densities. Bearing in mind that from the unpolarized data $G_2(Q_0^2) \sim 0.45$ one has that $\Delta G_1(Q_0^2)$ should be smaller than 0.9. This fact could be critical for the validity of the BBS model if more precise data are available in the future.

The BBS polarized $x(\Delta f(x) + \Delta \bar{f}(x))$ distributions at $Q_0^2 = 4 \text{ GeV}^2$ are shown in Fig. 3. In Fig. 4 we compare our results for the BBS *unpolarized* $x(f(x) + \bar{f}(x))$ input densities (solid curves) with the MRS(A') set of unpolarized parton distributions (dashed curves) at the same $Q_0^2 = 4 \text{ GeV}^2$. The difference between the BBS unpolarized input parton densities and the MRS(A') ones is somewhat greater than the usual difference between the various sets of unpolarized parton distributions used in the literature. The difference for $x(u + \bar{u})$ and $x(d + \bar{d})$ quarks increases up to 20% depending on x , while *e.g.*, for MRS(D0') and MRS(A') set of input valence quark densities it is typically 6-8% in the x range: $0.01 \leq x \leq 0.50$ and amounts to 15-20% for the range: $0.5 < x \leq 0.7$. As one can see from Fig. 4 the agreement for the sea quarks and the gluons is better, of the same quality as for the well known different sets of unpolarized input partons.

(b) *Models based on the unpolarized parton densities*

Let us continue now with discussion of our results of the fit to the data using for the input polarized parton densities the set (35). Such a set of input partons had been used in [23], but starting at very small $Q_0^2 = 0.34 \text{ GeV}^2$.

Unlike the BBS model the data do not allow to determine η_s , the first moment of the polarized sea, in proper way if the parametrization (35) is used. In other words, if η_s is taken to be a free parameter, its value determined from the fit to $A_1^N(x, Q^2)$

data, does not agree with the experimental value of $\eta_s/3 = -0.10 \pm 0.02$ [9]. That is why we fix η_s from the measured value of $\Gamma_1^p(5 \text{ GeV}^2) = 0.141 \pm 0.011$ to be $\eta_s = -0.290$ at $Q_0^2 = 4 \text{ GeV}^2$.

As already mentioned above it is impossible to determine accurately the form of the polarized gluon density from these data alone and therefore additional constraints have to be applied to the gluonic input parameters. As in [32] we have used the assumption $a_g = a_s$ which defines the behaviour of $\Delta G(x, Q^2)$ at small x . It turns out that even in that case it is not possible to determine by the fit the value of the parameter b_g in (35) which controls the behaviour of $\Delta G(x, Q^2)$ at large x . For that reason the fit to the data was performed at different fixed values of b_g in the range $0 \leq b_g \leq 7$. Further, if a_d is left as a free parameter, its best-fit value is negative independently of the value of b_g in the above range. This fact, presumably reflects the circumstance discussed in Section 2, namely that from the data in the small x region $g_1^p - g_1^n > g_1^p + g_1^n$, which probably induces such a behaviour in $\Delta d_v(x, Q_0^2)$. For this negative value of a_d : $a_d \sim -0.13$

$$\frac{|\Delta d_v(x)|}{d_v(x)} = 0.339 A_d x^{a_d}$$

is greater than 1 at very small x : $x < 0.3 \cdot 10^{-6}$ and the positivity condition (8) is broken. In addition, the corresponding value of a_s determined by this fit is such that the positivity condition (8) for $\Delta Sea(x)$ is violated too, but at large x : $x > 0.80$. That is why we have taken $a_d = 0$, the smallest value of a_d which guarantees positivity for Δd_v at all x . The change of χ^2 from $\chi^2(a_d < 0) \cong 215$ to $\chi^2(a_d = 0) \cong 220$ is negligible.

The results of the fit to $A_1^N(x, Q^2)$ data are presented in Table 1.

Table 1. The results of the NLO QCD fit to the world A_1^N data using the set (35) for the input polarized partons ($a_d = 0$).

	$b_g = 0$	$b_g = 5$	$b_g = 7$
χ^2/DOF	221.2/200	220.5/200	219.5/200
a_u	0.196 ± 0.018	0.178 ± 0.027	0.169 ± 0.025
a_s	0.892 ± 0.085	0.706 ± 0.155	0.694 ± 0.112
η_g	-0.14 ± 0.26	1.07 ± 0.70	1.29 ± 0.53

Although only three free parameters $\{a_u, a_s, \eta_g\}$ have been used a very good description of the data is achieved. This is illustrated in Figs. 2a - 2f (dashed curves),

which show the NLO description of the various A_1^N measurements. In Fig. 7 we compare our NLO results for $g_1^N(x, Q^2)$ with the SMC data. The input polarized parton distributions (35) are shown in Fig. 5. The value of χ^2/DOF is 220.5/200 for $b_g = 5$ and practically does not depend on b_g (see the Table). This value is better than that one in the case of the BBS model. The mean value of η_g , the first moment of the polarized gluon density, is sensitive to the value of b_g : η_g increases with increasing b_g . The values of η_g at $b_g \geq 5$ are greater than 1 and are in agreement with those determined by the NLO analysis in [32]. The sets of polarized quark densities corresponding to gluons with $b_g = 5$ and $b_g = 7$ are practically the same.

We have found also that values for η_g smaller than 1, and even a small negative value $\eta_g = -0.14 \pm 0.26$ corresponding to $b_g = 0$, are not excluded by the data. In the last case, however,

$$\frac{|\Delta Sea(x)|}{Sea(x)} = 1.12x^{0.892}$$

and positivity is violated in the large x region: $x > 0.88$.

In Fig. 6 a comparison between the BBS input polarized distributions (30) and the polarized densities (35) is shown. It is seen that while the distributions $x(\Delta u + \Delta \bar{u})$ and $2x\Delta \bar{s} = 2x\Delta \bar{q}$ are very similar for these two parametrizations, the polarized distributions $x(\Delta d + \Delta \bar{d})$ and $x\Delta G$ corresponding to (30) and (35) differ considerably, $x(\Delta d + \Delta \bar{d})$ for $x > 0.35$ and $x\Delta G$ for all x . The polarized gluon distribution enters $g_1(x, Q^2)$ at next-to-leading order and bearing in mind the accuracy of the present data these different gluon contributions can not be distinguished. However, the difference between $x(\Delta d + \Delta \bar{d})(x, Q_0^2)$ leads to a considerably different behaviour of $A_1^d(x, Q^2)$ in the kinematic region: $x > 0.35$, $Q^2 \sim 5 - 10 \text{ GeV}^2$, and allows a better fit to the SLAC E143 data on $A_1^d(x, Q^2)$ in this region in the case of the parametrization (35) for the input polarized parton densities. The difference for $x(\Delta d + \Delta \bar{d})$ at large x is a consequence of the fact that the BBS distributions are forced to satisfy (25) as $x \rightarrow 1$.

5. Conclusion

We have performed a next-to leading order QCD analysis (\overline{MS} scheme) of the world data on polarized deep inelastic lepton-nucleon scattering. The QCD predictions have been confronted with the directly measured virtual photon-nucleon asymmetry $A_1^N(x, Q^2)$ rather than with the polarized structure function $g_1^N(x, Q^2)$ derived from the data by different additional procedures. Different parametrizations for the input

polarized parton densities have been examined: the Brodsky, Burkardt and Schmidt model and a model based on unpolarized parton densities. In the BBS model the positivity constraints for the unpolarized parton densities are automatically valid. In the second one it is easy to control them. In both cases a good fit to the data is achieved. The description of the data is slightly better if for the input polarized parton distributions the second parametrization is used.

A distinctive feature of the BBS model is that the helicity-dependent input parton distributions $f_{\pm}(x, Q_0^2)$ (rather than $\Delta f(x, Q_0^2)$ and $f(x, Q_0^2)$) are parameterized so that the polarized, as well as the unpolarized data have to be fitted by the same parameters (34). This feature creates a serious challenge to the model. We have shown that the BBS model is compatible with the present DIS data although the agreement with the MRS(A') parametrization of the unpolarized parton distributions at $Q^2 = 4 \text{ GeV}^2$ is somewhat worse than the usual level of agreement between the different sets of the input unpolarized parton densities usually used in the literature. Our result for the axial charge $a_0(5 \text{ GeV}^2) = \Delta\Sigma(5 \text{ GeV}^2) = 0.341$, obtained in the BBS model is in a good agreement with its experimental value $a_0(5 \text{ GeV}^2) = 0.29 \pm 0.06$ recently determined from a combined analysis of all proton, neutron and deuteron data, while using the second parametrization for the input polarized densities this quantity is not well determined from the fit to the data. This results from the fact that the sea quark distributions are still largely undetermined if the second kind of parametrization is used.

The present polarized data do not allow a precise determination of the shape of the polarized gluon density. It follows from our fits that values of $\Delta G_1(4 \text{ GeV}^2)$, the first moment of the polarized gluon density, both greater and smaller than 1, are possible. Negative values of ΔG_1 are not excluded either.

Despite the great progress of the past few years it is clear that in order to test precisely the spin properties of QCD more accurate DIS polarized data at fixed x and various Q^2 are needed. In addition, charged current data will be very important for a precise determination of the polarized parton densities and especially, for a precise flavour decomposition of the polarized quark sea. Finally, a direct measurement of $\Delta G(x, Q^2)$ in processes such as J/ψ production in lepton-hadron scattering with a polarized beam will answer the important question about the magnitude and the sign of ΔG_1 .

Acknowledgments

We are grateful to O. V. Teryaev for useful discussions and remarks.

This research was partly supported by a UK Royal Society Collaborative Grant, by the Russian Fund for Fundamental Research Grant No 95-02-04314a, by the INTAS Grant No 93-1180 and by the Bulgarian Science Foundation under Contract Ph 510.

References

- [1] M. J. Alguard et al., Phys. Rev. Lett. **41** (1978) 70;
G. Baum et al., Phys. Rev. Lett. **51** (1983) 1135.
- [2] EMC, J. Ashman et al., Phys. Lett. **B206** (1988) 364;
Nucl. Phys. **B328** (1989) 1.
- [3] E. Leader and M. Anselmino, Z. Phys. **C41** (1988) 239.
- [4] SLAC E142, D. L. Anthony et al., Phys. Rev. Lett. **71** (1993) 959;
- [5] SLAC E143, K. Abe et al., Phys. Rev. Lett. **74** (1995) 346.
- [6] SLAC E143, K. Abe et al., Phys. Rev. Lett. **75** (1995) 25.
- [7] SLAC E143, K. Abe et al., Phys. Lett. **B364** (1995) 61.
- [8] SMC, D. Adams et al, Phys. Lett. **B329** (1994) 399;
erratum *ibid* **B339** (1994) 332.
- [9] SMC, D. Adams et al, CERN preprint PPE/97-22, 1997, hep-ex/9702005.
- [10] SMC, D. Adeva et al, Phys. Lett. **B302** (1993) 533.
- [11] SMC, D. Adams et al, Phys. Lett. **B357** (1995) 248.
- [12] SMC, D. Adams et al, Phys. Lett. **B396** (1997) 338.
- [13] E. B. Zijlstra and W. L. van Neerven, Nucl. Phys. **B147** (1994) 61;
R. Mertig and W. L. van Neerven, Z. Phys. **C70** (1996) 637;
W. Vogelsang, Phys. Rev. **D54** (1996) 2023.
- [14] Particle Data Group, L. Montanet et al, Phys. Rev. **D50** (1994) 1173;
F. E. Close and R. G. Roberts, Phys. Lett. **B313** (1993) 165.
- [15] G. R. Farrar and D. R. Jackson, Phys. Rev. Lett. **35** (1975) 1416.
- [16] F. E. Close and D. Sivers, Phys. Rev. Lett. **39** (1977) 1116.
- [17] S. J. Brodsky, M. Burkardt and I. Schmidt, Nucl. Phys. **B441** (1995) 197.
- [18] A.D. Martin, R.G. Roberts and W.J. Stirling, Phys. Lett. **B354** (1995) 155.
- [19] R. D. Ball, S. Forte and G. Ridolfi, Nucl. Phys. **B444** (1995) 287.

- [20] J. Batrels, B. I. Ermolaev and M. G. Ryskin, Z. Phys. **C70** (1996) 273;
DESY preprint 96-025, hep-ph/9603204.
- [21] NMC, P. Amaudruz et al., Phys. Lett. **B295** (1992) 159;
M. Arneodo et al., Phys. Lett. **B364** (1995) 107.
- [22] L. W. Whitlow et al., Phys. Lett. **B250** (1990) 193.
- [23] M. Glück, E. Reya, M. Stratmann and W. Vogelsang, Phys. Rev. **D53** (1996)
4775.
- [24] D. B. Stamenov, Mod. Phys. Lett. **A10** (1995) 2029.
- [25] W. Buck and F. Gross, Phys. Rev. **D20** (1979) 2361;
M. Z. Zulhof and J. A. Tjon, Phys. Rev. **C22** (1980) 2369;
M. Lacombe et al., Phys. Rev. **C21** (1980) 861;
R. Machleidt et al., Phys. Rep. **149** (1987) 1.
- [26] G. Parisi and N. Surlas, Nucl. Phys. **B151** (1979) 421;
I. S. Barker, C. B. Langensiepen and G. Shaw, Nucl. Phys. **B186** (1981) 61.
- [27] V. G. Krivokhizhin et al., Z. Phys. **C36** (1987) 51; *ibid* **C48** (1990) 347.
- [28] J. Ellis and R. L. Jaffe, Phys. Rev. **D9** (1974) 1444; *Erratum* **10** (1996) 1669.
- [29] R. D. Ball, S. Forte and G. Ridolfi, Phys. Lett. **B378** (1996) 255.
- [30] M. Glück, E. Reya and W. Vogelsang, Nucl. Phys. **B351** (1991) 579.
- [31] R. Blankenbecler and S.J. Brodsky, Phys. Rev. **D10** (1974) 2973;
J. Gunion, Phys. Rev. **D10** (1974) 242;
G. Farrar, Nucl. Phys. **B77** (1974) 429.
- [32] T. Gehrmann and W. J. Stirling, Phys. Rev. **D53** (1996) 6100.

Figure Captions

Fig. 1. Comparison of the SMC data [9, 12] on $g_1^p \pm g_1^n$ as function of x at mean value $Q^2 = 10 \text{ GeV}^2$.

Fig. 2a-2f. Comparison of our NLO results for $A_1^N(x, Q^2)$ with the present data. The solid and dashed curves are the best fits to the data corresponding to the BBS model (30) and parametrization (35) of input polarized parton distributions, respectively.

Fig. 3. Next-to-leading order input polarized parton distributions at $Q^2 = 4 \text{ GeV}^2$ in the BBS model ($x\Delta u \equiv x\Delta u + x\Delta\bar{u}$ and $x\Delta d \equiv x\Delta d + x\Delta\bar{d}$).

Fig. 4a-b. Comparison between BBS *unpolarized* parton distributions (solid curves) and MRS(A') set of unpolarized parton densities (dashed curves) at $Q^2 = 4 \text{ GeV}^2$ ($xu \equiv xu + x\bar{u}$ and $xd \equiv xdu + x\bar{d}$).

Fig. 5. Next-to-leading order input polarized parton distributions at $Q^2 = 4 \text{ GeV}^2$ corresponding to parametrization (35) in the text ($a_d = 0$, $b_g = 7$).

Fig. 6. Comparison between the input polarized parton distributions in the BBS model (solid curves) and parametrization (35) (dashed curves). $xu \equiv xu + x\bar{u}$, $xd \equiv xdu + x\bar{d}$ and $2x\Delta s = 2x\Delta\bar{q}$.

Fig. 7. Comparison of our NLO results for $g_1^N(x, Q^2)$ with SMC data [9, 12] at the measured Q^2 . The solid curves correspond to BBS model and dashed ones to parametrization (35) of the input polarized parton densities.

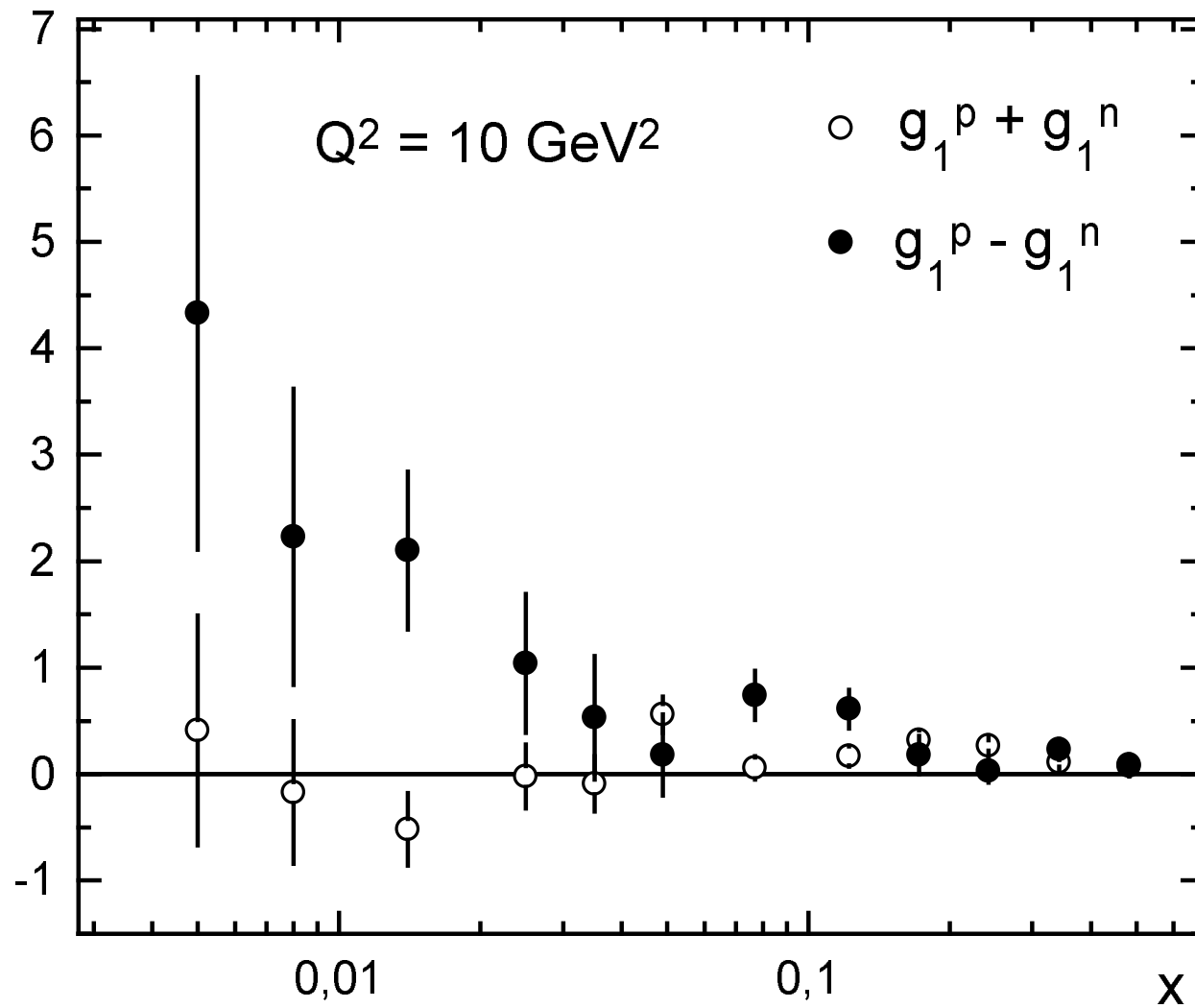


Fig. 1.

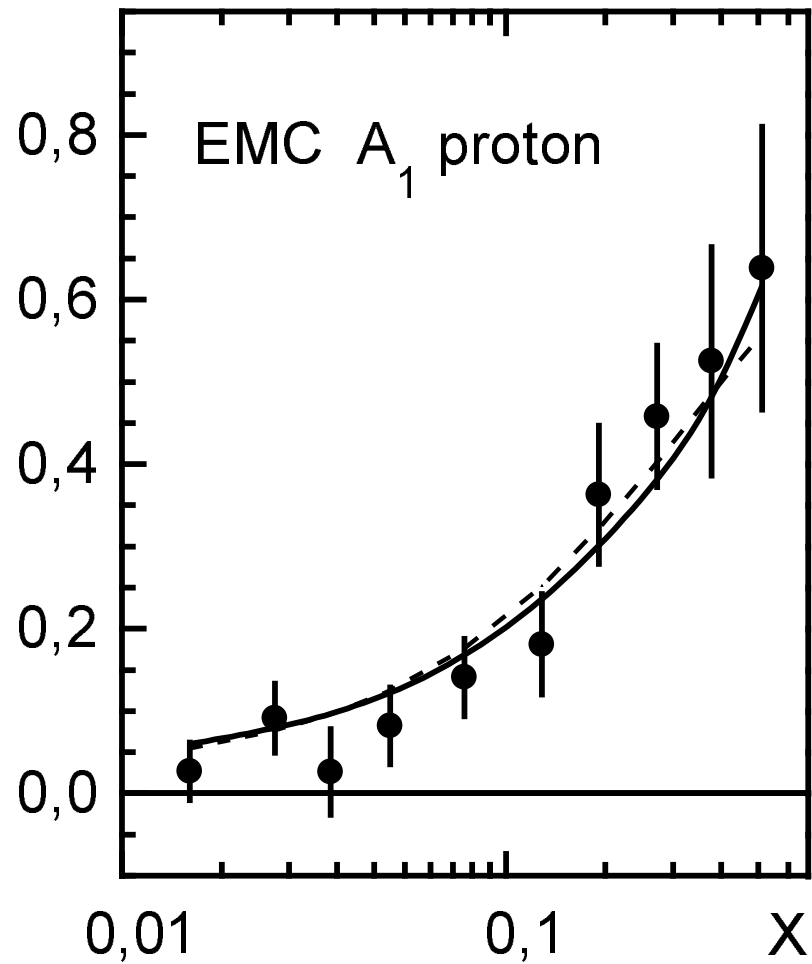


Fig. 2a

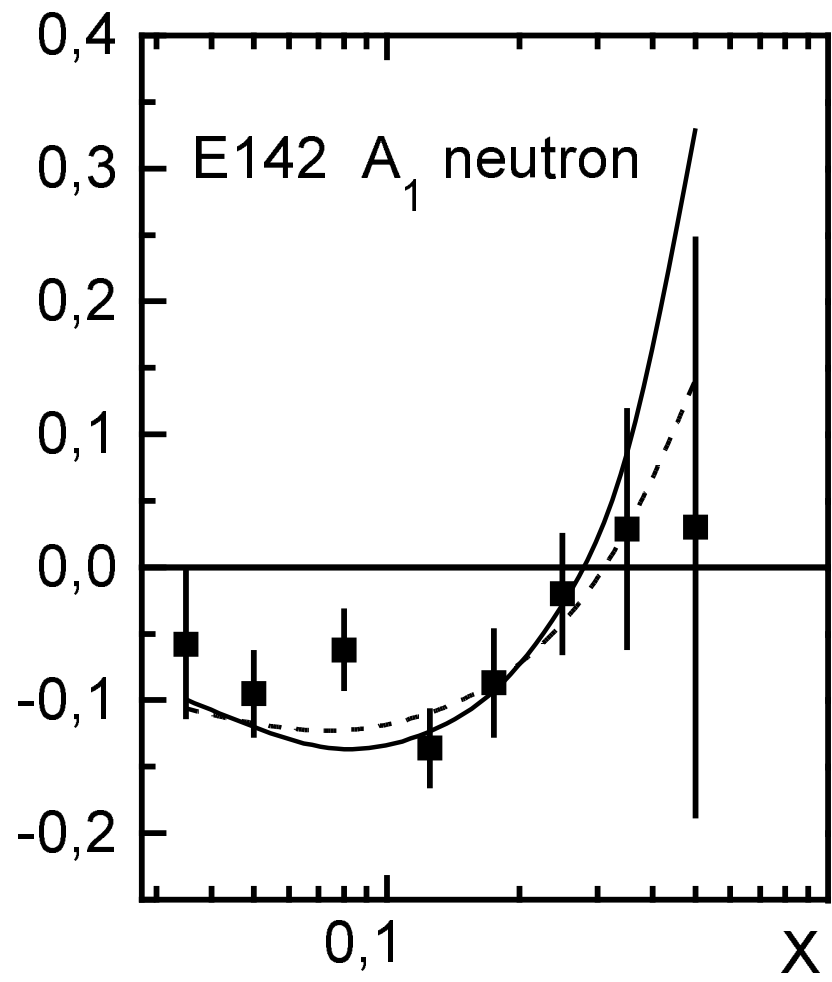


Fig. 2b

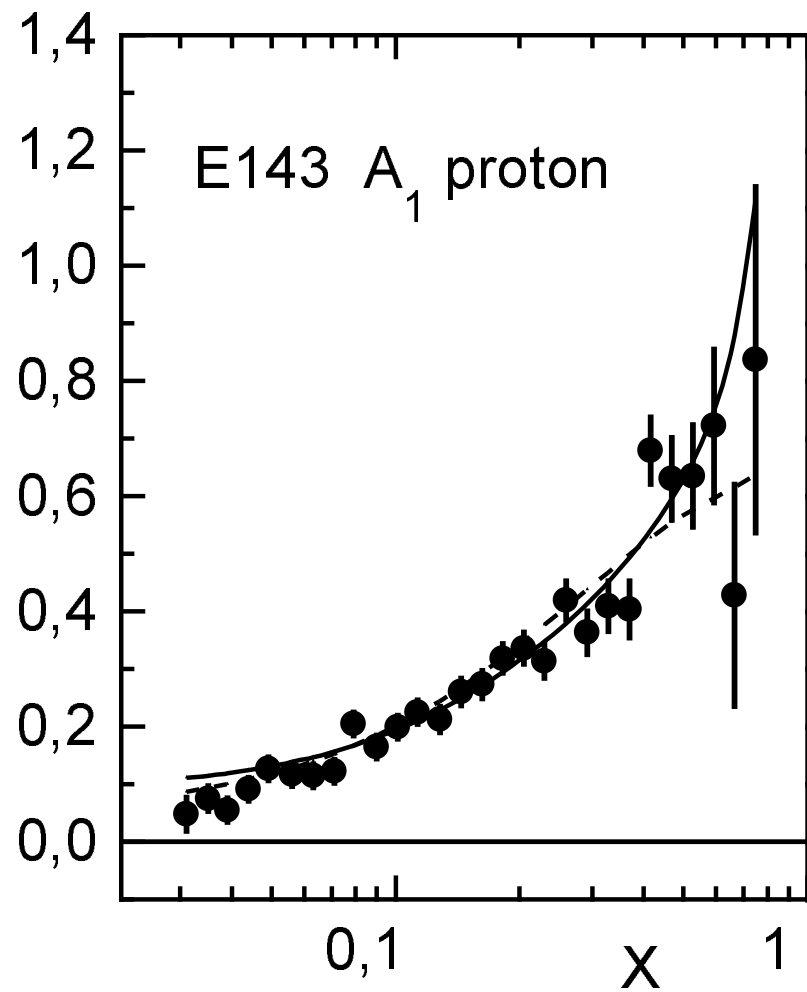


Fig. 2c

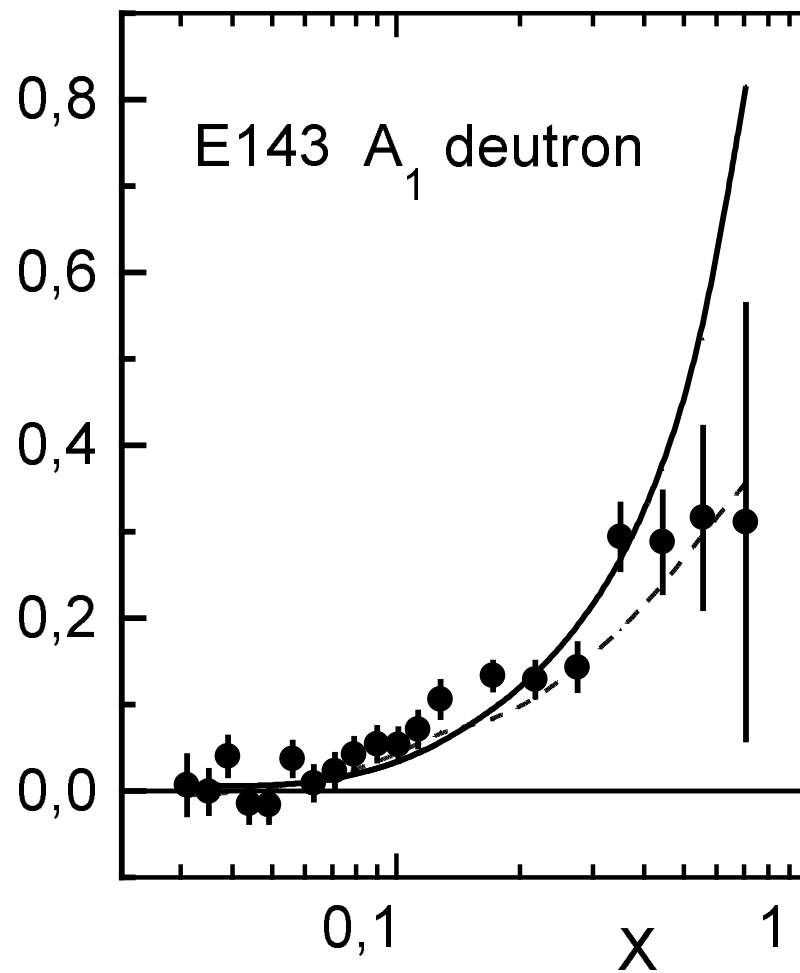


Fig. 2d

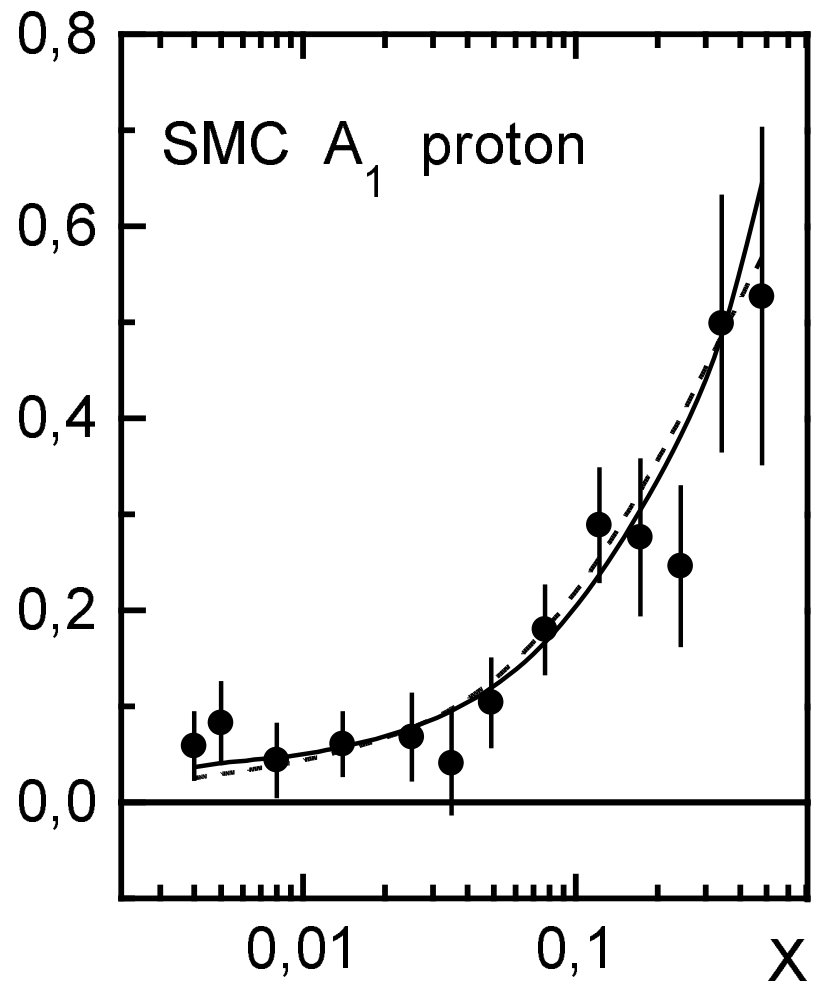


Fig. 2e

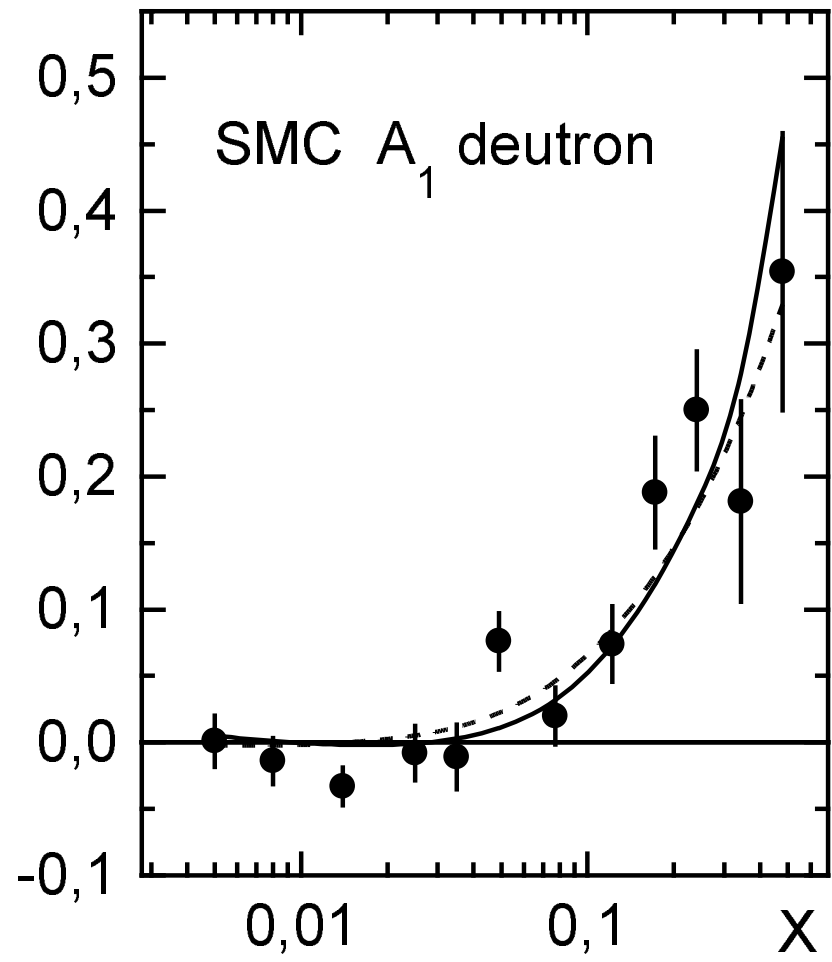


Fig. 2 f

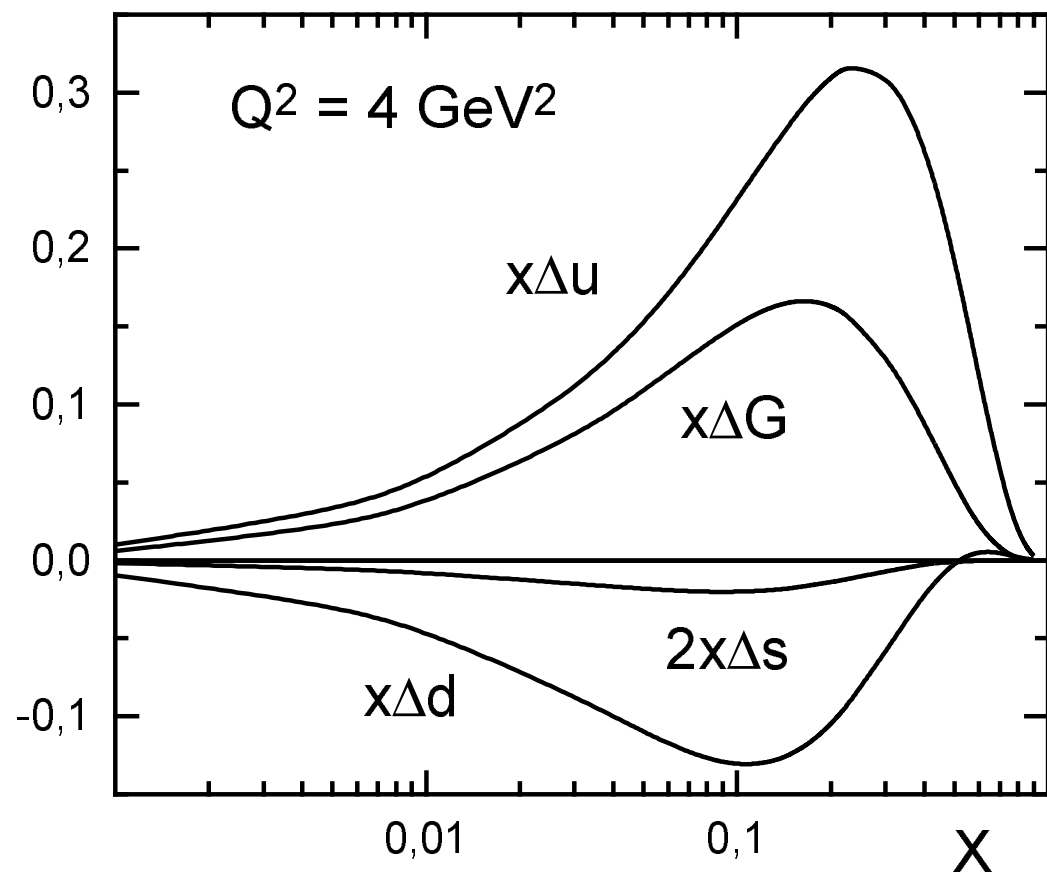


Fig. 3

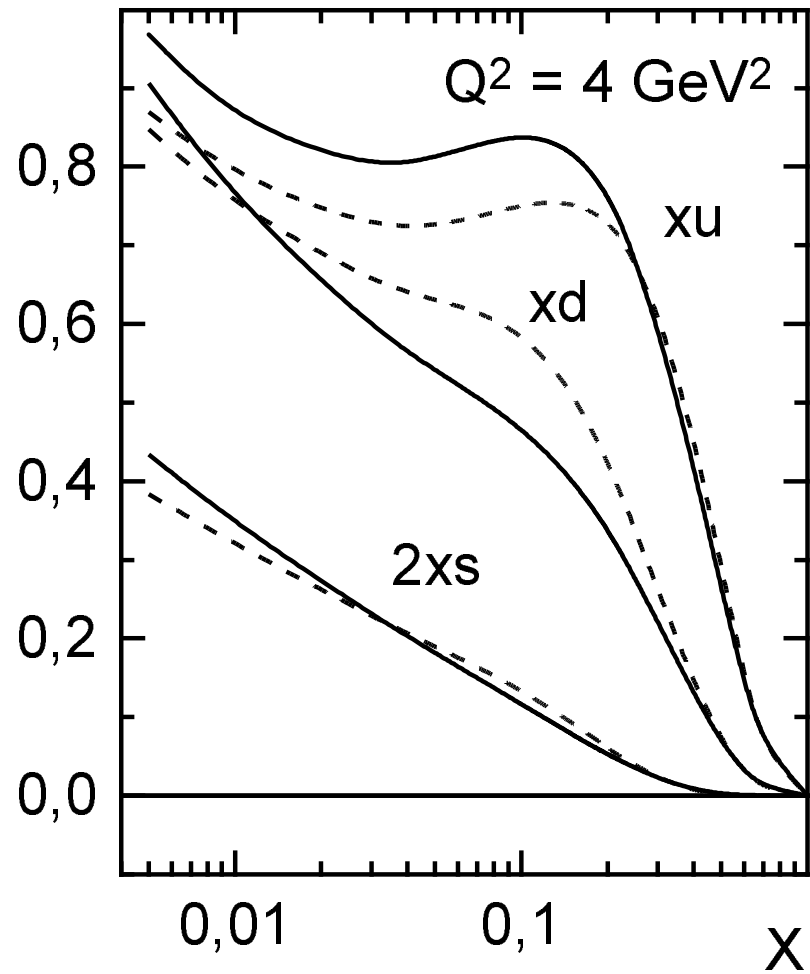


Fig. 4a

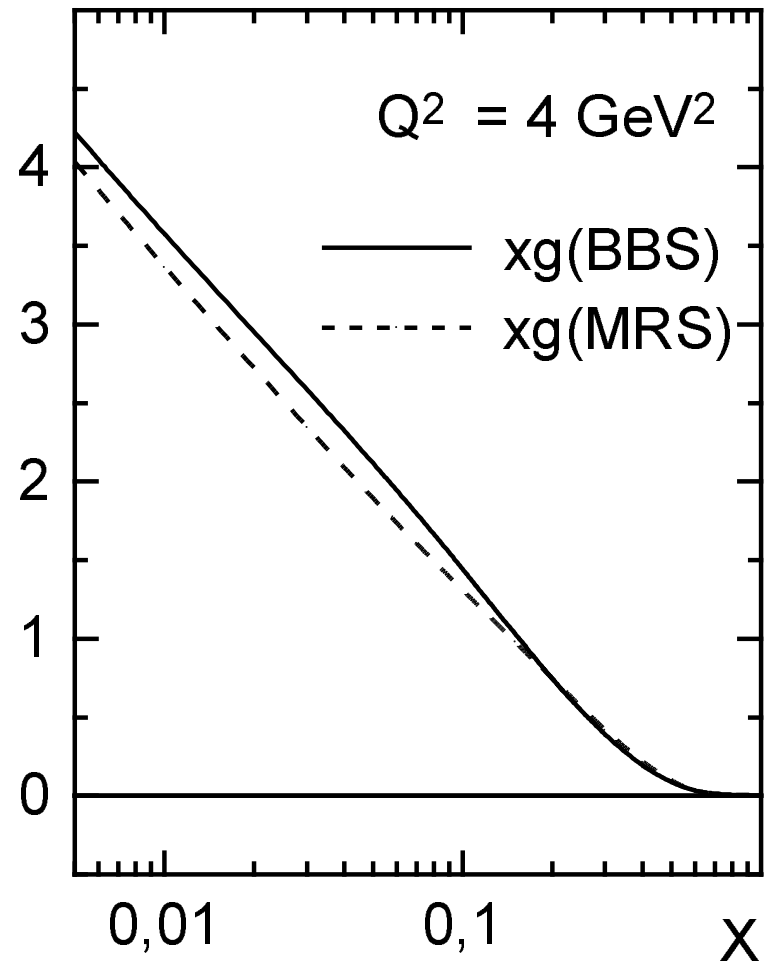


Fig. 4b

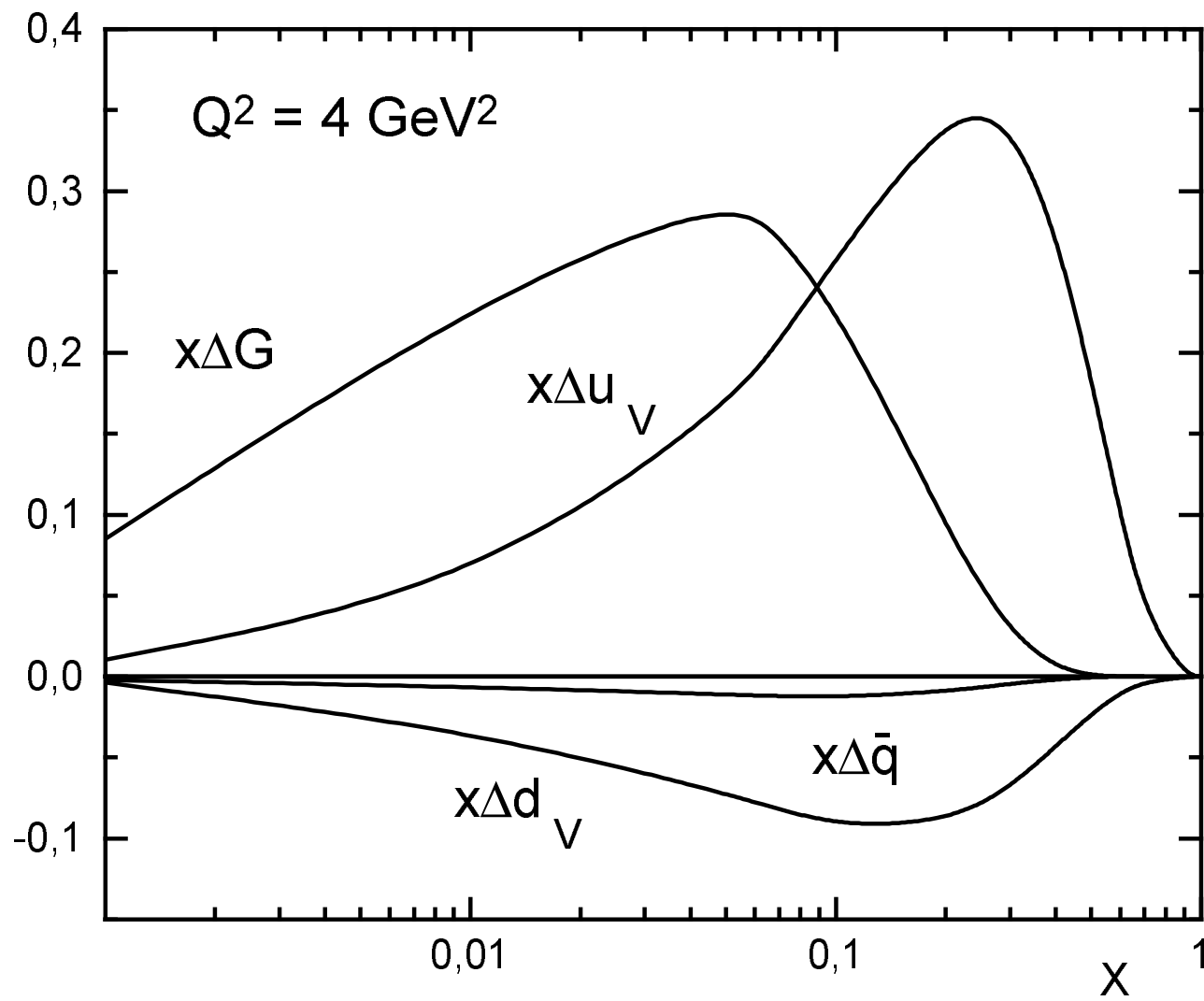


Fig. 5.

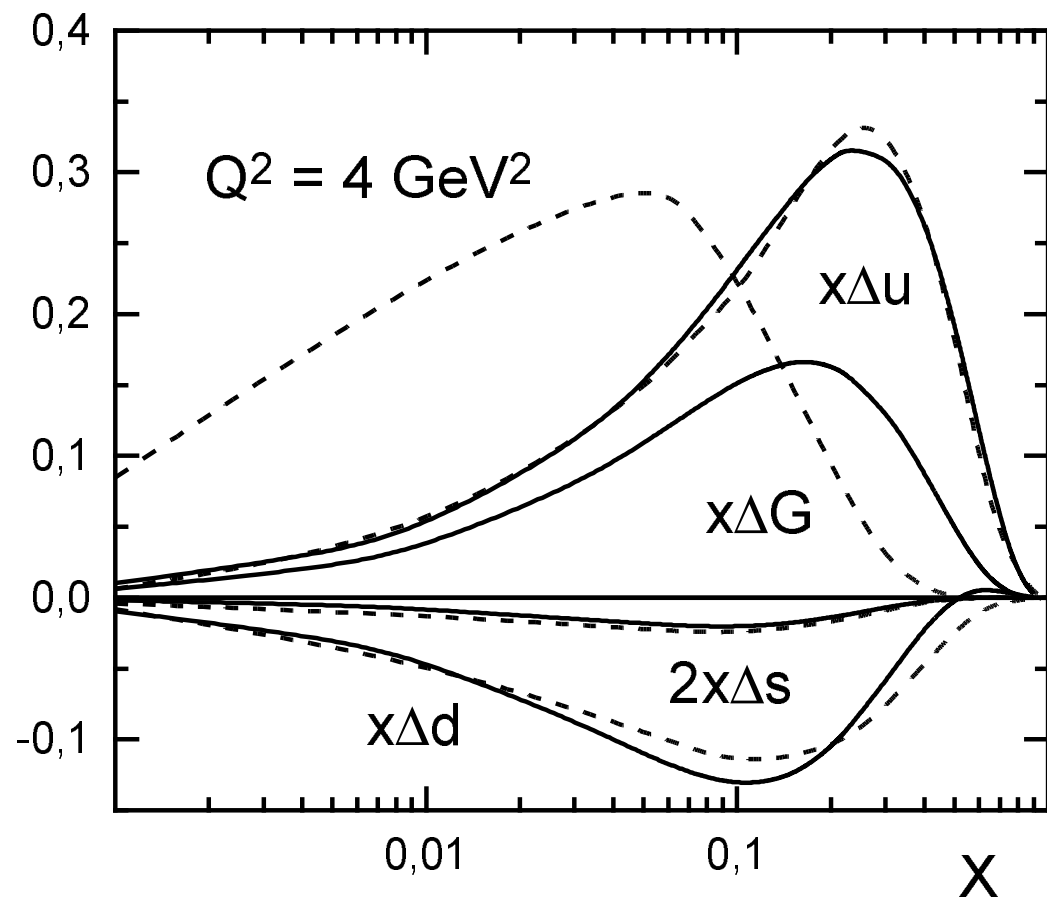


Fig. 6

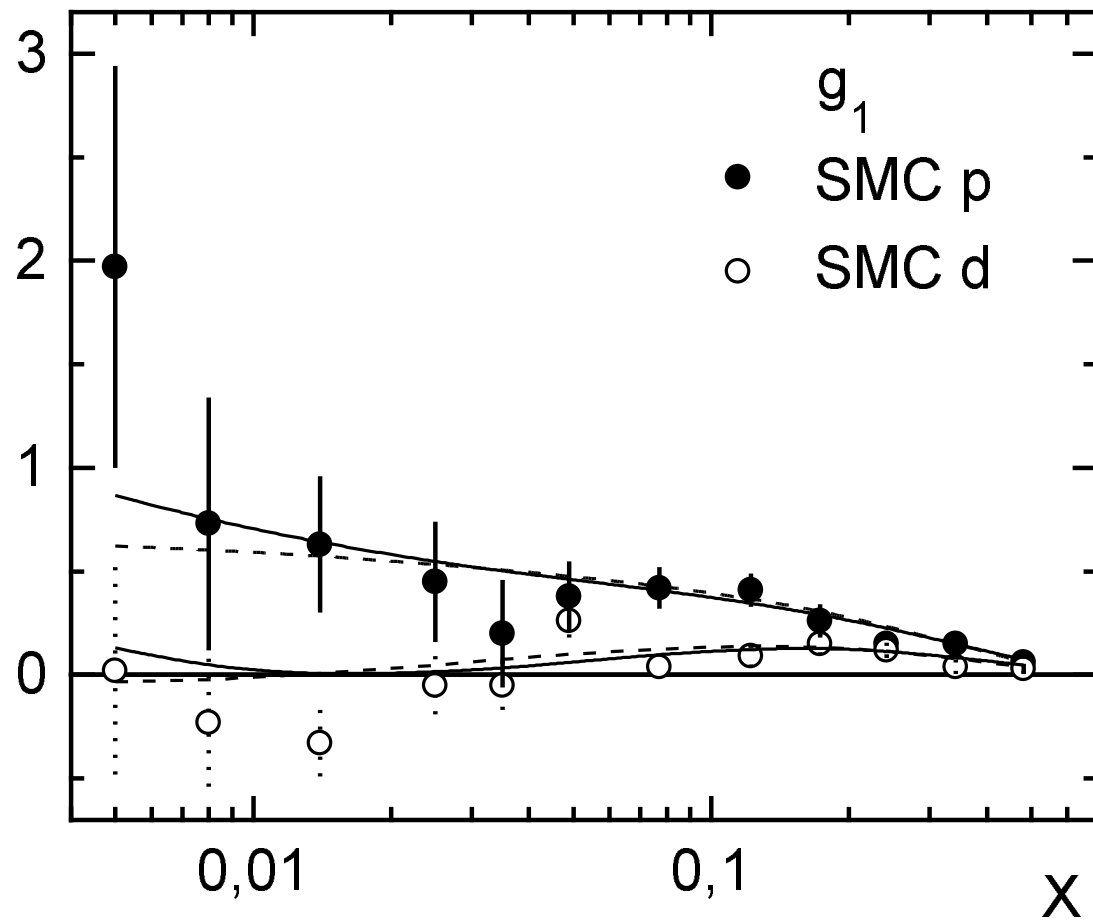


Fig. 7